Int J Adv Manuf Technol (2016) 87:3185–3193
DOI 10.1007/s00170-016-8723-0

ORIGINAL ARTICLE

A servo-motor driven active blank holder control system for deep drawing process

De'an Meng[1] · **Shengdun Zhao**[1] · **Lei Li**[2] · **Chen Liu**[1]

Received: 17 November 2015 / Accepted: 4 April 2016 / Published online: 12 April 2016

Abstract A novel active blank holder control system driven by a servo-motor for deep drawing is proposed and designed in this paper. In contrast to most published works utilizing complicated hydraulic systems, this new device has a simpler mechanical structure and ensures more complex blank holder force (BHF) trajectory. An elastomer is employed in this system, and the BHF can be controlled by changing the servo-motor speed actively. To obtain an accurate and robust control performance against punching speed variation, a fuzzy logic controller is developed. Then, the whole control structure is applied to a Matlab real-time workshop to perform the BHF tracking tasks. Finally, experimental hardware is constructed and the constant, sinusoidal, and pulsating BHF trajectory tracking tasks are performed. Conducted results indicate that the proposed system can supply a robust and accurate blank holder force.

Keywords Blank holder force · Servo-motor · Active control · Fuzzy control

1 Introduction

Deep drawing is a primary sheet forming operation to make automobile panels and other thin-walled parts. The forming quality is affected by many factors, including part geometry, material properties, lubricating condition as well as the blank holder force (BHF), and a good control of these parameters can delay the failure of the part. Particularly, among all these factors, the BHF which controls the material flowing into the die cavity plays a critical role in producing a well-drawn part. Many studies have shown that [1–3] an insufficient BHF tends to cause wrinkling of the drawn part. However, an excessive BHF may cause tear. In many cases, a variable blank holder force (VBHF) that the BHF varies over the punch stroke is favorable for drawing.

A lot of research work has been reported to investigate the effect of VBHF on product quality. Traversin and Kergen [4] proposed a closed-loop system to supply VBHF. They suggested that the VBHF could avoid wrinkling and increase the drawing ratio in comparison with a constant BHF. Cao and Boyce [5] monitored the tendency of wrinkling and tearing and thereby designed a single variable binder force trajectory for a conical cup forming using numerical tools. Chengzhi [6] presented a new optimization algorithm integrating the finite-element method (FEM) and adaptive response surface methodology (ARSM) to determinate the optimum BHF. Wang [7] integrated a proportional-integral-derivative (PID) controller into the FEM code to conduct the closed-loop forming simulation of a step rectangle box, through which the optimal BHF trajectories were determined for each separated binder. Kitayama [8] applied the radial basis function (RBF) on sequential approximate optimization to calculate the optimal VBHF trajectory. Simulation using finite element method is an effective way to obtain a proper BHF trajectory.

To acquire a proper BHF, many devices have been proposed to control the BHF. Siegert [9] introduced a hydraulic drawing mechanism used in a single-action press and made it possible to control the distribution of blank holder pressure through the punch stroke. The hydraulic drawing mechanism named hydraulic die-cushion was widely used in drawing

✉ De'an Meng
flymendel@163.com

[1] School of Mechanical Engineering, Xi'an Jiaotong University, Xi'an, Shaanxi 710049, Peoples Republic of China

[2] Department of Mechanical Engineering, University of Alberta, Edmonton, AB T6G 2G8, Canada

process in later stage. In comparison to the hydraulic die-cushion integrated with the press, Gunnarsson [10] developed a new blank holder system with degressive gas springs which was independent of press facilities. He examined that the new system could obtain degressive, constant, and progressive BHF trajectories. Yagami [11] employed a total of 108 segment blank holding hydraulic actuators to control the material flow. Yun [12] proposed a new method to control the BHF using an MR damper for the first time, and a closed-loop control system was developed in his study. In addition, Tommerup [13] presented a special hydraulic system integrated into existing drawing tools without modifying the press. Instead of simply increasing or decreasing the BHF, Yagami [14] controlled blank holder motion to couple with the punch stroke; his works showed a proper blank holder movement that can prevent tear and improve the part formability. Some researchers [15–17] also superposed oscillation on the blank holder with a dedicated device. Their works suggested that a pulsating BHF is benefit for deep drawing.

Devices and control methods mentioned above are based on hydraulic or pneumatic actuators; the problems of control delay, oil leakage, and complexity of the system are difficult to manage. Besides, the servo mechanical press is gradually replacing the hydraulic press for its high controllability and efficiency [18]. The traditional method supplying BHF with pneumatic or hydraulic actuators is unsuitable for the development of servo presses. In recent years, the servo-motor is used to supply a constant BHF during drawing processing. Qin [19] discussed the feasibility of using servo-motor to supply BHF in theory, and he considered that servo die-cushion would cost little energy if the blank holder did not move a lot during drawing process. He also designed a new BHF device with six-bar linkage mechanism driven by a servo-motor [20], and the device could supply a variable BHF. Kriechenbauer [21] presented a servo-screw press which was equipped with a servo die-cushion, and the servo die-cushion was driven by eight motors. Although all of the devices above were driven by servo-motor, the control method was usually in a passive way that the servo-motor worked as a torque motor. In that situation, the high precision and controllability of the servo-motor was not fully used.

This paper demonstrates an active blank holder control system for deep drawing using a servo-motor. To buffer the impact and improve the control performance, an elastomer is employed in this system. In order to achieve a better control effect, a dynamic model of the system is established and a fuzzy logic controller is developed. The active blank holder control system is examined in an Instron 5900 testing machine which serves as a servo press with different drawing speed. The results show that the active blank holder control system has a very good and robust performance for the control of BHF.

2 Mechanical design and modeling

2.1 Mechanical design

The drawing cushion, driven by a servo-motor, can be named servo die-cushion. Figure 1 shows the principle of a conventional servo die-cushion used in a drawing press [22]. In this figure, the blank holder and the screw are connected rigidly. During a drawing procedure, the slide drives the blank holder moving downwards, and the servo-motor rotates reversely along with the screw providing a torque to generate BHF. Thus, the operation of this cushion is similar to that of hydraulic cushions. In most cases, the BHF is controlled in a passive way. Additionally, the BHF can be controlled linearly by the motor torque, as shown in Fig. 2. However, BHF has a dead zone due to the friction. To constrain the dead zone size, the reduction ratio between servo-motor and screw should be as small as possible. This leads to the servo-motor operating at a low speed, which will result in torque fluctuations. Under the circumstance of BHF controlled passively, the control precision does not achieve a satisfactory level and a good speed and position control of the servo-motor is not obtained either.

To acquire an accurate BHF, an active blank holder control system is proposed in this paper, and it is composed of an actuator system and a control system. Figure 3 shows a schematic of the mechanical working principle of the actuator system. The actuator system consists of a screw, elastomer, pin, guide sleeve, servo-motor, planetary reducer, and other parts. The force can be produced by a servo-motor and delivered to the blank holder through the screw, guide sleeve, elastomer, and pin one by one. The system contains several actuators according to actual situation, and each actuator can be independently driven, which can supply a VBHF which varies through the punch stroke. The planetary reducer and the elastomer are vital components for the actuator system. The planetary reducer with a high reduction ratio ensures the servo-

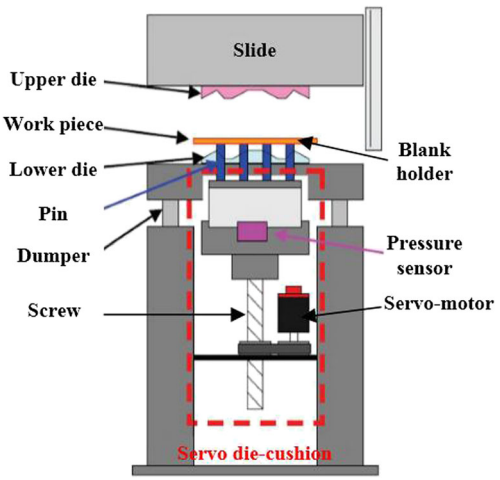

Fig. 1 Schematic of a conventional servo die-cushion

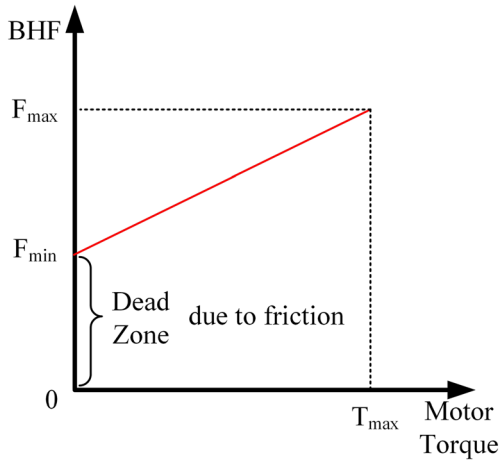

Fig. 2 Relationship between BHF and motor torque

motor working at high speed, and the elastomer has two functions: one is to buffer the impact; the other is to improve the control performance. The elasticity of the elastomer should be properly selected according to the max BHF. In this paper, a spring with small elasticity is regarded as the elastomer for convenience in the latter experiment.

Figure 4 shows the simplified motion sequence of the die-cushion proposed in this article. First, the press slide moves downwards. The moment the upper die contacts the blank, the die-cushion is pre-accelerated. The elastomer reduces the slide impact on the blank. Afterwards, the blank is clamped between the upper tool and the blank holder. Then a drawing process is conducted, and the blank holder provides a suitable BHF varying through the punch stroke. After a drawing process is finished, the die-cushion moves upwards to lift the drawn part. At the stage of 2–3, BHF should strictly follow the scheduled trajectory especially when forming complex parts. The biggest challenge for the system is an accurate and dynamical control of the force, despite movement of the die-cushion. In deep drawing process driven by a servo press, to obtain a fine-produced part, the punch speed is always changing over the punch stroke according to a certain scheme. Under such circumstance, a standard PI BHF controller may fail if the drawing speed changed drastically. Further mechanical analysis needs to be conducted to acquire an accurate and robust controller.

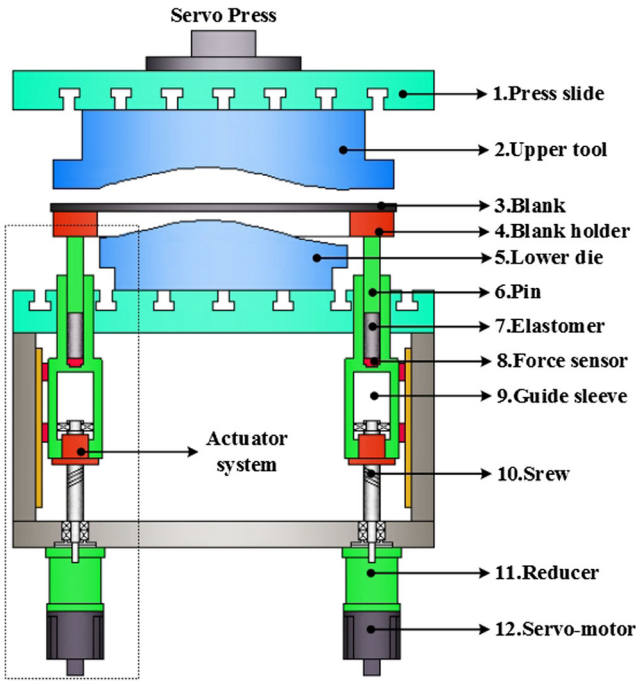

Fig. 3 The principle of the actuator system

2.2 System modeling analysis

The actuator configuration is shown in Fig. 5. Using the second Newton's law and principles of actuator system, the BHF can be described by the following equation:

$$F = ES_t \frac{(L-L_0)}{L_0} + ma + f \tag{1}$$

Here, E is the elastomer elastic modulus, S_t is the elastomer cross-sectional area, L and L_0 are elastomer length before and after a deformation, respectively, m is the blank holder mass, a is the blank holder acceleration, and f is the friction force between pin and guide sleeve.

Take a derivation on both sides of Eq. (1), we can get the motion equation of the BHF

$$\frac{dF}{dt} = \frac{ES_t}{L_0}[v_1(t)-v_2(t)] + m\ddot{v}_1(t) + \dot{f} \tag{2}$$

where $v_1(t)$ and $v_2(t)$ denote the velocity of the upper die and guide sleeve, respectively. The upper die velocity is associated with servo press which cannot be changed by the die-cushion. The two latter items of Eq. (2) also cannot be altered by the blank holder system. Guide sleeve velocity is the only factor controlled by the die-cushion which can change the BHF. The relationship between guide sleeve speed and servo-motor speed is as follows:

$$v_2(t) = P\omega(t)/(2\pi i_n) \tag{3}$$

in which P is the screw lead, i_n is the gear ratio of the reducer, and $\omega(t)$ is the servo-motor rational speed. Substituting Eq. (3) into Eq. (2), we obtain Eq. (4) as follows:

$$F = \frac{ES_t}{L_0}\int_0^t \left[v_1(t)-\omega(t)\frac{P}{2\pi i_n}\right] + m\dot{v}_1(t) + f(v_1) \tag{4}$$

$\omega(t)$ can be estimated by referring to the field-oriented control theory of the modern AC machines; the motion equation of the servo-motor can be expressed as follows:

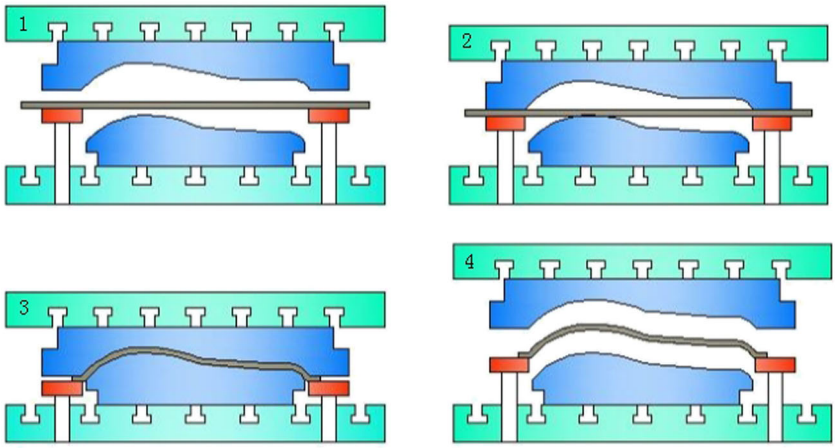

Fig. 4 Simplified motion sequence of the die-cushion. *1* Slide accelerates. *2* Upper die contacts the blank. *3* Drawing process. *4* Eject drawn part

$$\begin{cases} J\dfrac{d\omega}{dt} = T_e - \omega B_\omega + T_L \\ T_e = 1.5\ P_n \psi_f i_q \\ T_L = \dfrac{FP}{2\pi} \end{cases} \tag{5}$$

where J is the equivalent moment of inertia in the drive system, T_e is the electric torque, T_L is the load torque, B_ω is the viscous friction coefficient, P_n is the number of pole pairs, i_q is the stator q-axis current, ψ_f is the flux linkage induced by the permanent magnets in the stator, F is the BHF, and P is the screw lead.

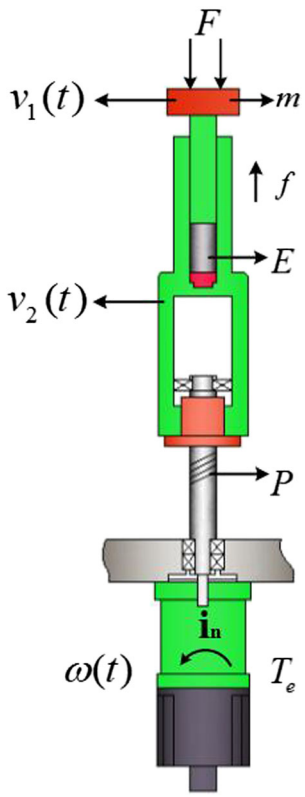

Fig. 5 Structure of the actuator

From Eq. (4) and Eq. (5), one can see that the BHF could be controlled by the servo-motor speed which is relevant to the input current. In other words, the objective of the control is to generate the input current to regulate the BHF to the pre-defined value. The control strategy can be described as follows: when the actual BHF detected by the force sensor exceeds the scheduled value, the servo-motor should accelerate to make the elastomer release and decrease the BHF. When the actual BHF is less than the pre-defined value, the guide sleeve should decelerate to compress the elastomer and increase the BHF. However, the elastomer cross-sectional area *St*, friction force *f*, and the upper die speed $v_1(t)$ are variable and an impulsive load exists in the beginning and end of a drawing process. The actuator system is time-varying, nonlinear, and uncertain. It will be difficult to establish an accurate mathematical model between BHF and motor input current.

3 Control of the BHF

As discussed above, strict model-based control methods may not be conveniently applied. Alternatively, following the intuitive control of human operator, a fuzzy control could be more appropriate [23, 24].

Figure 6 shows a block diagram of the control system, and it contains two controllers: fuzzy BHF controller (FFC) and motor speed controller (MSC). The FFC calculates the difference and the corresponding change between the reference BHF and the actual BHF. Then, emulating a human operator, it infers a required speed correction applied to the scheduled speed of the blank holder. As shown, the inner-loop is a speed tracking system with reference speed as its input and armature current as its output. The MSC is programmed in the motor driver with the PID controller. The reference BHF could be acquired through experimental and finite element method. Generally, the reference BHF is variable through the punch stroke. The scheduled speed is referred to the stamping speed, and it can be measured by a grating scale.

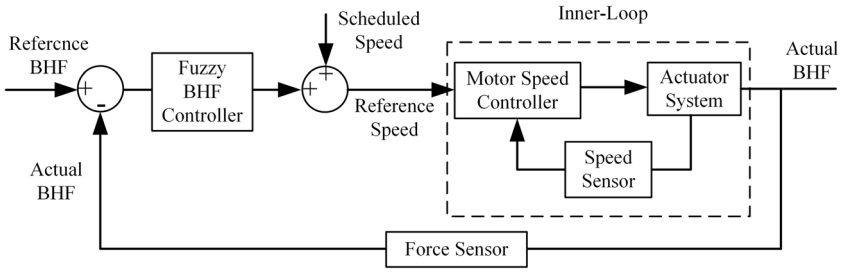

Fig. 6 Block diagram of the control system

Figure 7 shows the structure of the fuzzy BHF controller. It consists of two input variables and one output variable. Error e denotes the difference between the reference BHF and the actual one, change in error de represents the change in the current difference, and output $\Delta\omega$ is the speed correction inferred each time. Error e and change in error de can be described by the following equation:

$$e = \text{scheduled BHF} - \text{actual BHF} \tag{6}$$

$$de = \text{present error} - \text{previous error} \tag{7}$$

The error input variable has five triangular membership functions, and the change in error input has three triangular membership functions. All the input variables are defined in the universe of discourse [−1, 1], as shown in Fig. 8. The output variable is composed of seven triangular membership functions with universe of discourse [−1, 1] as seen in Fig. 8. In addition to this paper, since the fuzzy controller has rich nonlinear characteristics of mapping, scaling factors of input and output signals is used to adjust the control characteristics of the fuzzy controllers for the dynamic characteristics of the controlled system. Three scaling factors K_e, K_{de}, and K_u are introduced to produce normalized input and output signals of the fuzzy logic controller as seen in Fig. 7.

The output of the control rules is the control output $\Delta\omega$, which is defined as $\Delta\omega = f(e, de)$. Table 1 gives the employed 15 control rules that are extracted and generalized from the experiences of skilled human operators. For instance, the first rule in Table 1 indicates that when the BHF error is negative big (NB) meaning that the actual BHF has increased significantly higher than its previous value, the controller then applies an NB correction to the set-point speed of the controlled stand to increase the guide sleeve speed, thereby reducing BHF. It is noted that the control rules in Table 1 also incorporate the change of error. The varying tendency of the current error, as a second input, refines the speed corrections, especially around the equilibrium. Therefore, very likely, an even better BHF controller than the operator control may be attained. In the defuzzification, min-max implication functions and centroid method are used. Thus, the speed correction is generated at each control cycle by

$$\Delta\omega = K_u \frac{\sum_{i=1}^{n} u_i \mu(u_i) du}{\sum_{i=1}^{n} \mu(u_i) du} \tag{8}$$

where K_u is the scaling factor of the speed correction, u is the real-valued control signal determined by the domain, and (u_i) is the memberships of the selected fuzzy control actions.

On top of that, when the motor rotation direction changes, it will cause system fluctuations for the reason of a system backlash. It is necessary to restrict motor rotation only in one direction. The control strategy can be described by the following equation:

$$\omega = \begin{cases} 0\ , & \omega < 0 \\ \omega\ , & other \\ \omega_{max}, & \omega > \omega_{max} \end{cases} \tag{9}$$

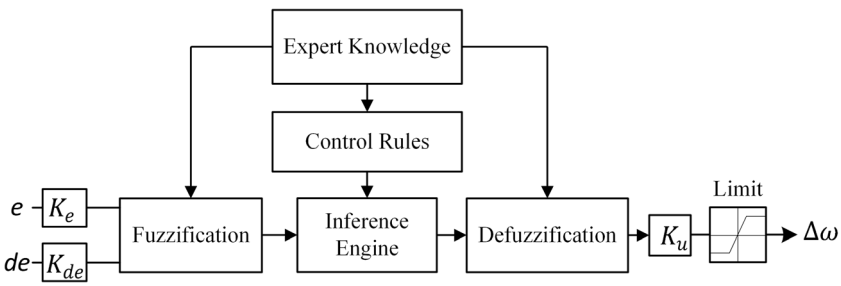

Fig. 7 Overview of the fuzzy BHF controller

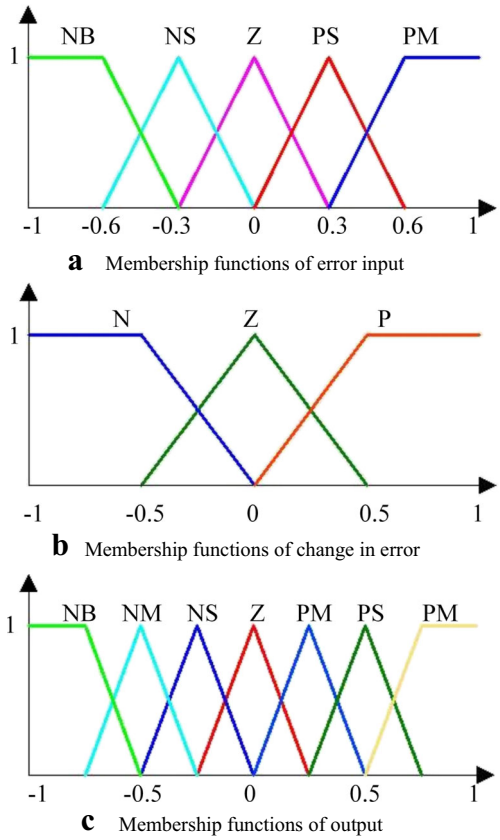

Fig. 8 Membership functions. **a** Membership functions of error input. **b** Membership functions of change in error. **c** Membership functions of output

4 Experimental evaluation

To test the performance of the active blank holder control system designed, as well as to experimentally validate its theoretical model and perform closed-loop force control experiments, the experimental setup illustrated in Fig. 9 has been developed. The experimental setup is a scaling-down model in consideration of costs and convenience. An Instron 5900 testing machine containing a displacement and force sensor is used as a servo press, and the punch speed could be changed and programmed. The BHF could be measured by the force sensor. A spring whose coefficient is 40 N/mm is regarded as the elastomer. The associated lists are tabulated in Table 2.

In this setup, a PC augmented with a PCI-1711 data acquisition card is used in the closed-loop experiments. This card

Table 1 Fuzzy controller rule base

Output		Error				
		NB	NS	Z	PS	PB
Change in error	N	NB	NM	NS	PS	PB
	Z	NB	NM	Z	PM	PB
	P	NB	NS	PS	PM	PB

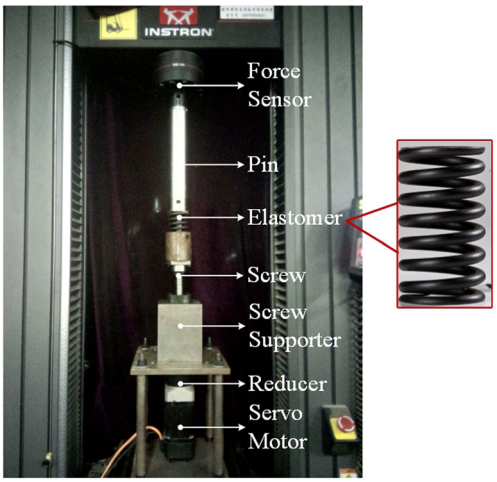

Fig. 9 Experimental apparatus

provides an interface between the Matlab Real Time Toolbox and the system and sends or receives signals pertaining to the force, displacement, and velocity. Also, the system is controlled by command blocks in the Matlab Real Time Toolbox, which cooperates with a PCI-1710 card where hardware support-generated output signals are implemented enabling real-time control over the experiment. All the data were sampled at a sampling frequency of 100 Hz. The control platform implemented in the Matlab/Simulink environment runs on an Intel i3 3.3 GHz PC with 8.0 GB memory.

In an actual press, the movement of the press slide is analogous to a sine-wave form. However, the Instron testing machine only can be controlled by the speed. To acquire a sine-wave movement trajectory, the punch curve is divided into four parts with independent speed, as shown in Fig. 10. In this paper, the four kinds of punching speed are 20, 15, 10, and 5 mm/s. Each speed is employed for 2 s, and the total drawing depth is 100 mm.

The control parameters of the fuzzy BHF controller and MSC are selected as the following:

Fuzzy BHF controller: $K_e = 0.2$, $K_{de} = 1$, $K_u = 10$
Motor speed controller: $K_P = 0.2$, $K_I = 1$, $K_D = 0$

Table 2 The devices used and corresponding parameters

Name	Parameters
Instron 5900	Maximum pressure: 100 kN
Spring	Coefficient: 40 N/mm
Reducer	Gear ratio: 32
Servo-motor	Rated power: 0.75 kW, Rated speed: 3000 r/min
Acquisition card	Model: Advantech PCI-1711
Screw	Lead: 25 mm Diameter: 25 mm

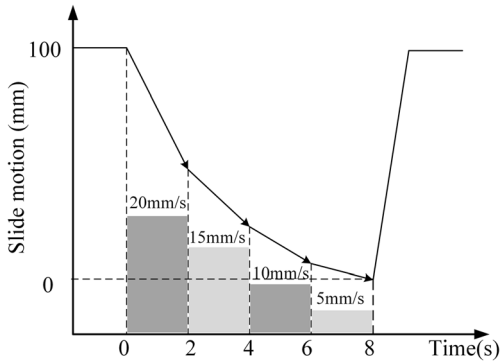

Fig. 10 Movement diagram of the press slide

5 Results and discussion

For the verification of the proposed system, three different BHF trajectories are employed in the test: constant, sinusoidal, and pulsating BHF trajectories.

In the case of testing constant BHF trajectory, the BHF is set to a constant value which is $F_r = 500$ N. The punching speed follows the law shown in Fig. 10. At the time 2, 4, and 6 s, the punching speed decreases sharply and an impact is introduced to the system. Because of the elastomer between the servo-motor and the blank holder, the impact can be well absorbed. Applying the proposed control method, the system responds quickly, and the servo-motor works stably. The responses of the BHF and the tracking error are shown in Fig. 11. As seen in this figure, the fuzzy BHF controller has a perfect tracking performance. At the beginning, it needs more time to achieve the referenced value. This is because we restrict the servo-motor to run only in a single direction. When the BHF error is NB, the controller generates a NB correction to reduce the servo-motor speed. Under that circumstance, the servo-motor speed usually turns to zero. That means the increase of BHF totally depends on the movement of the upper die. After the BHF reaches the set value, the BHF can track the referenced value very well. Even the punching speed changes; only small chattering occurs. The tracking error of the whole process is always less than 2.5 N. The system has a high precision in controlling the constant BHF.

The sinusoidal BHF trajectory is a common BHF control method in the drawing process. It can supply a variable blank hold force which can improve the formability. In this case, both the punching speed and the scheduled BHF are variable, which leads to complicated control tasks. The sinusoidal function used in this test is defined as

$$F_r = 250 * \sin\left(\frac{\pi}{4}t - \frac{\pi}{2}\right) + 250 \tag{10}$$

Applying the same controller, response of the system and tracking error are shown in Fig. 12. The punching speed also follows the law shown in Fig. 10. At the time 2, 4, and 6 s, the BHF does not show significant fluctuation. However, the tracking error is greater than that in the constant BHF case. From Fig. 12, we can see that the tracking error during the time 0–4 s is more stable than that in the period of 4–8 s. The reason for this phenomenon is that the output factor K_u, whose value is 10, is suitable for the punching speed during time 0–4 s and turns out to be too large for the time 4–8 s. The maximum tracking error appears in the position of peaks and valleys. This is mainly because the MSC used here was a universal product. When the load changes, motor speed is prone to distort in the position of peaks and valleys. But in this experiment, the MSC is accurate enough to control the BHF. If a higher control precision is needed, the speed controller should be optimized using some advanced control algorithm (like sliding mode control). During the whole experiment, the system has a good performance in the control of the BHF. No matter how the reference BHF and punching speed change, the tracking error can be controlled within 5 N. The result of tracking a sinusoidal BHF trajectory is acceptable.

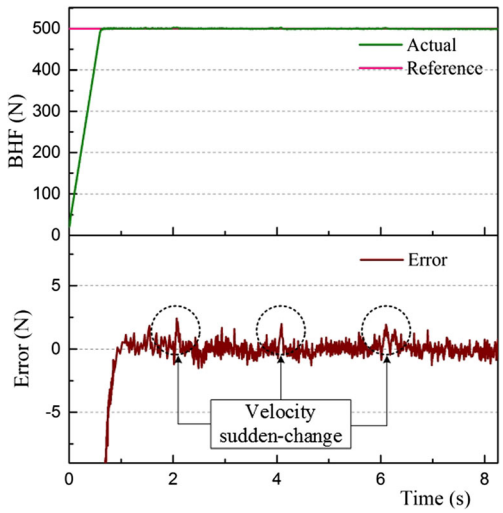

Fig. 11 Constant BHF response and tracking error

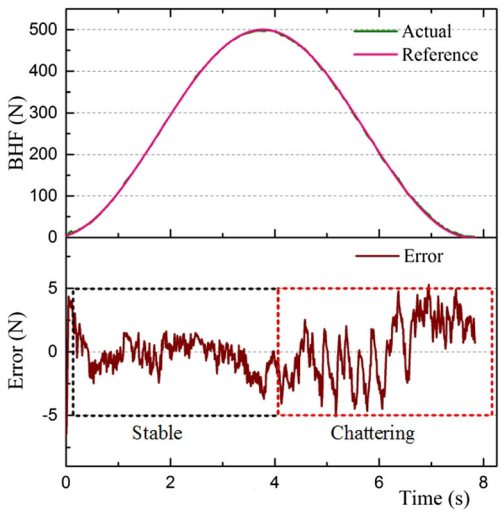

Fig. 12 Sinusoidal BHF response and tracking error

A pulsating BHF is proved to improve the drawability, as compared with a static constant BHF. In this paper, a pulsating BHF trajectory is tested. The pulsating BHF is described as follows:

$$F_r = 50*\sin(\pi t + \pi) + 500 \quad (11)$$

From Eq. (11), we can see that the pulsating trajectory is the combination of a constant signal and a sinusoidal signal. The pulsating BHF trajectory changes fast. Correspondingly, the system needs to respond quickly. The response and tracking error are shown in Fig. 13. In this case, the tracking error has some regular law. At the peaks and valleys, the tracking error reaches larger values. The reason for this is the same with what we discussed in the sinusoidal trajectory. However, the maximum error of the whole stamping procedure still does not exceed 5 N. The active blank holder control system provides excellent tracking performance.

Furthermore, Fig. 14 shows the result of the system without an elastomer and planetary inducer (as shown in Fig. 1), in which the BHF is controlled in a passive way. That means the servo-motor works in a reverse rational mode, and the BHF is generated by a resistance torque. A parabolic trajectory is examined in the passive BHF control system. From the results, we can see that a strong irregular pulsation exists in the response of the BHF, and the maximum BHF error exceeds 30 N. The passive control accuracy is much worse than the active control method.

Figures 11, 12, and 13 show that the proposed system has an excellent dynamical performance in the control of BHF, and the control accuracy is satisfactory. When the punching speed changes rapidly, the system can cushion the impact through the elastomer. From the experiments above, we know that the elastomer makes a great contribution to the system robustness. The tracking error in Fig. 11 is smaller than that in Figs. 12 and 13. The dynamic performance of the system can

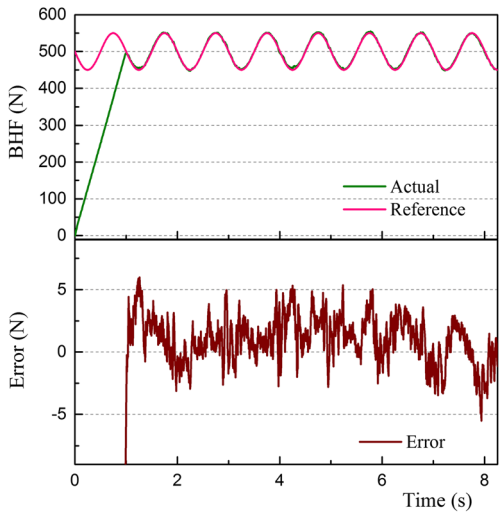

Fig. 13 Pulsating BHF response and tracking error

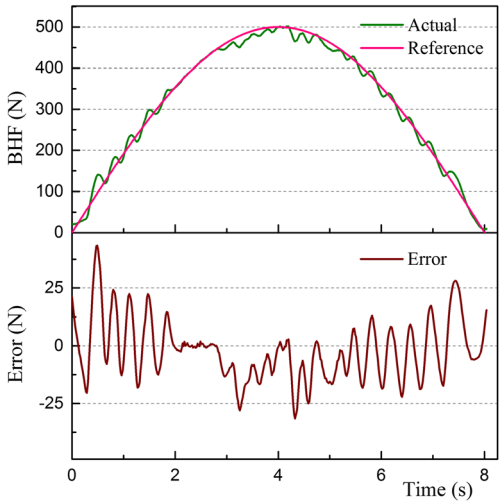

Fig. 14 Passive control response and tracking error

be further optimized, which will be studied in our future research. Comparing the result in Fig. 14 generated by a passive way, the active blank holder control system is obviously superior than the conventional one. The major contribution of this system presented in this paper is the application of the elastomer. After employing an elastomer, the BHF can be altered in an active way via changing the motor speed. In order to obtain a better control effect, it is preferred to employ a planetary reducer with a large reduction ratio. In that way, the servo-motor can work in a high speed, and the torque pulsation can be avoided greatly. The elastic coefficient of the elastomer has an important effect on the control performance of the system. In this paper, a spring is used as an elastomer. Due to its low elastic coefficient, the BHF can only be changed in a small range. When larger BHF is needed, the rubber or other objects with a greater elastic coefficient can serve as the elastomer, and the control algorithm should be updated correspondingly.

6 Conclusions

In this paper, an active blank holder control system has been proposed and designed for drawing presses to retain a variable BHF during drawing operations, and its feedback control characteristic has been experimentally evaluated. The developed system has a simple mechanical structure which is driven by a servo-motor. Mathematical analyses confirm that the servo-motor speed has a strong relation with the BHF. A fuzzy BHF controller is proposed and employed to resist the stamping load disturbance and speed variation. The constant, sinusoidal, and pulsating BHF trajectory tracking tasks indicate that the control system can supply a robust and accurate BHF. This paper is the base of our future attempts in the development of a large-load BHF system for industrial applications.

References

1. Obermeyer EJ, Majlessi SA (1998) A review of recent advances in the application of blank-holder force towards improving the forming limits of sheet metal parts. J Mater Process Technol 75(1):222–234
2. Modi B, Kumar D (2013) Development of a hydroforming setup for deep drawing of square cups with variable blank holding force technique. Int J Adv Manuf Technol 66(5-8):1159–1169
3. Kitayama S, Hamano S, Yamazaki K, Kubo T, Nishikawa H, Kinoshita H (2010) A closed-loop type algorithm for determination of variable blank holder force trajectory and its application to square cup deep drawing. Int J Adv Manuf Technol 51(5-8):507–517
4. Traversin M, Kergen R (1995) Closed-loop control of the blank-holder force in deep drawing: finite-element modeling of its effects and advantages. J Mater Process Technol 50:306–317
5. Cao J, Boyce MC (1997) A predictive tool for delaying wrinkling and tearing failures in sheet metal forming. J Eng Mater Technol 119(4):354–365
6. Chengzhi S, Guanlong C, Zhongqin L (2004) Determining the optimum variable blank-holder forces using adaptive response surface methodology (ARSM). Int J Adv Manuf Technol 26:23–29
7. Wang WR, Chen GL, Lin ZQ (2007) Determination of optimal blank holder force trajectories for segmented binders of step rectangle box using PID closed-loop FEM simulation. Int J Adv Manuf Technol 32:1074–1082
8. Kitayama S, Kita K, Yamazaki K (2012) Optimization of variable blank holder force trajectory by sequential approximate optimization with RBF network. Int J Adv Manuf Technol 61(9-12):1067–1083
9. Siegert K, Doege E (1993) CNC hydraulic multipoint blankholder system for sheet metal forming presses. CIRP Ann Manuf Technol 42(1):319–322
10. Gunnarsson L, Asnafi N, Schedin E (1998) In-process control of blank holder force in axi-symmetric deep drawing with degressive gas springs. J Mater Process Technol 73(1):89–96
11. Yagami T, Manabe K, Yang M et al (2004) Intelligent sheet stamping process using segment blankholder modules. J Mater Process Technol 155:2099–2105
12. Yun YW, Bae HS, Park MK (2010) A study of the control of the blank holding force using an MR damper in a drawing press. J Mech Sci Technol 24(11):2281–2288
13. Tommerup S, Endelt B (2012) Experimental verification of a deep drawing tool system for adaptive blank holder pressure distribution. J Mater Process Technol 212(11):2529–2540
14. Yagami T, Manabe K, Yamauchi Y (2007) Effect of alternating blank holder motion of drawing and wrinkle elimination on deep-drawability. J Mater Process Technol 187:187–191
15. Ali S, Hinduja S, Atkinson J et al (2008) The effect of ultra-low frequency pulsations on tearing during deep drawing of cylindrical cups. Int J Mach Tool Manuf 48:558–564
16. Mostafapur A, Ahangar S, Dadkhah R (2013) Numerical and experimental investigation of pulsating blankholder effect on drawing of cylindrical part of aluminum alloy in deep drawing process. Int J Adv Manuf Technol 69:1113–1121
17. Kitayama S, Natsume S, Yamazaki K, Han J, Uchida H (2016) Numerical investigation and optimization of pulsating and variable blank holder force for identification of formability window for deep drawing of cylindrical cup. Int J Adv Manuf Technol 82(1-4):583–593
18. Osakada K, Mori K, Altan T, Groche P (2011) Mechanical servo press technology for metal forming. CIRP Ann Manuf Technol 60(2):651–672
19. Qin S (2007) State-of-the-art of blank holding force control technology and feasibility of numerical servo-control holding. Zhongguo Jixie Gongcheng China Mech Eng 18(1):120–125
20. Qin S, Yang L, Yang B (2011) Blank holder force control system driven by servo-motor. Intell Control Autom 2(4):450
21. Kriechenbauer S, Mauermann R, Muller P (2014) Deep drawing with superimposed low-frequency vibrations on servo-screw presses. Procedia Eng 81:905–913
22. Altan T, Groseclose A (2009) Servo-drive presses-recent developments. Umformtechnisches Kolloqium Darmstadt 10
23. Tanaka K, Sugeno M (1992) Stability analysis and design of fuzzy control systems. Fuzzy Sets Syst 45(2):135–156
24. Lian RJ, Lin BF, Huang JH (2006) Self-organizing fuzzy control of constant cutting force in turning. Int J Adv Manuf Technol 29(5-6):436–445